Solid-State Chemistry

$Gd_5Si_2B_8$: A Ternary Rare-Earth-Metal Silicide Boride Compound**

Volodymyr Babizhetskyy, Jérome Roger, Stéphanie Députier, Roland Guérin, Régis Jardin, Josef Bauer, Kurt Hiebl,* Christophe Jardin, Jean-Yves Saillard, and Jean-François Halet**

In spite of the extensive experimental attention devoted to the various structural and physical properties of binary

[*] Dr. V. Babizhetskyy,[+] J. Roger, Dr. S. Députier, Prof. R. Guérin, Dr. R. Jardin, Dr. J. Bauer, Dr. C. Jardin, Prof. J.-Y. Saillard, Dr. J.-F. Halet
Laboratoire de Chimie du Solide et Inorganique Moléculaire
UMR 6511 CNRS-Université de Rennes 1
Institut de Chimie de Rennes
35042 Rennes (France)
Fax: (+33) 2-9963-5704
E-mail: guerin@univ-rennes1.fr
halet@univ-rennes1.fr

Prof. K. Hiebl
Institut für Physikalische Chemie
Universität Wien
Währingerstrasse 42, 1090 Wien (Austria)
Fax: (+43) 1-4277-9524
E-mail: kurt.hiebl@univie.ac.at

[+] present address:
FKF Max-Planck-Institute
Heisenbergstrasse 1, Postfach 800665, 70569 Stuttgart (Germany)

[**] V. Babizhetskyy is grateful to the Centre National de la Recherche Scientifique (CNRS, France) for a fellowship (2001–2002). We thank Dr. T. Roisnel (Centre de Diffractométrie, Rennes) for collecting X-ray diffraction data, M. Bohn (IFREMER, Brest) and J.-C. Jégaden (Centre de Microscopie à Balayage, Rennes) for the SEM and EPMA experiments. J.-F.H. and C.J. gratefully acknowledge the help of Dr. K. Costuas, Dr. R. Gautier, and S. Messaoudi (Rennes) for technical assistance. The authors acknowledge support from the Austrian (OAD)-French (Foreign Affairs Ministry) Amadeus exchange program (Project No. 10/2002, Grants No. 00064K and 03761XJ). K.H. thanks the MPI-CPFS Dresden (Germany), for the use of the SQUID magnetometer.

 DOI: 10.1002/ange.200352468

borides[1] and silicides[2] of the rare-earth metals (RE), there are comparatively few investigations of ternary silicide borides. Indeed, only a few boron-rich rare-earth metal silicide borides such as $RESiB_{44}$, $RESi_{4.6}B_{17.6}$, $RESi_{1.2}B_{41}$ (RE = Gd→Er, Y),[3] and $Tb_{3-x}C_2Si_8B_{36}$[4] containing icosahedral B_{12} cages, are known. This situation is in contrast with the ternary boride carbide phases of rare-earth metals which have received increasing attention over these last few years both experimentally and theoretically.[5] In an attempt to extend this chemistry to the RE-Si-B systems, we have explored different synthesis techniques, such as tin flux, and novel silicon-rich compounds, such as $Er_8Si_{17}B_3$, have thus been characterized.[6]

Herein we describe $Gd_5Si_2B_8$, a novel boron-rich rare-earth-metal silicide boride, which has been obtained from the peritectic reaction between the binary boride GdB_4 and silicide Gd_5Si_3. Indeed, the solid-state phase diagram of the ternary Gd-Si-B system established at 1270 K,[7] shows a thermodynamic equilibrium between $Gd_5Si_2B_8$ and the two binary compounds GdB_4 and Gd_5Si_3. In addition, numerous tie lines connect $Gd_5Si_2B_8$ to the other binary phases Gd_2B_5, Gd_5Si_4, and GdSi. Parallepiped-shaped single crystals of the ternary compound $Gd_5Si_2B_8$ could be extracted from solidified samples (arc melted and annealed in evacuated silica tubes at 1270 K for one month) and used for structure determination (Figure 1).[8] The structure shows that there are two crystallographically distinct gadolinium atoms (Gd1 and Gd2) and three types of boron atoms (B1, B2, B3). On the other hand, there is only one silicon position, which is not fully occupied ($\tau = 0.92(2)$). The structure of $Gd_5Si_2B_8$ can easily be described as an intergrowth of ThB_4-like[9] and U_3Si_2-like[10] slabs of compositions GdB_4 and Gd_3Si_2, respectively, alternating along the [001] direction. It can be considered as the topochemical sum $Gd_5Si_2B_8 = 2\,GdB_4 + Gd_3Si_2$.

The salient characteristics of the structure result from the occurrence of two independent, ordered, boron and silicon substructures. The silicon atoms within the U_3Si_2-like slab form Si–Si pairs with a Si–Si separation of 2.36(2) Å. These separations are consistent with those in binary U_3Si_2 (2.30 Å).[10] The boron atoms within the ThB_4-like slab form distorted B_6 octahedra, which are built from four basal B3 and two apical B2 atoms. These octahedra, which are inserted into gadolinium cubes, are close to ideal O_h symmetry, as shown by the intra-octahedral B2–B3 and B3–B3 distances which are quite similar (1.84(3) Å and 1.81(2) Å, respectively). B1–B1 units link four B_6 octahedra in the *ab* plane through B1–B3 bonds (Figure 1, bottom). Being linked to one B1 and two B3 boron atoms, every B1 boron atom is three-connected and adopts the sp^2-type coordination mode with bonding angles of 123(1)° for B3-B1-B1 and 113(2)° for B3-B1-B3.

The B1–B3 and B1–B1 bonds of 1.78(2) Å and 1.80(5) Å, respectively, are slightly shorter than the intra-octahedron distances. The B–B units ($z = 1/2$) and Si–Si pairs ($z = 0$) align on top of each other along the *c* direction. Finally, the Gd1 atoms are octahedrally surrounded by two boron and four silicon atoms, whereas the Gd2 atoms are twelve-coordinate, being bound by nine boron and three silicon atoms in a rather complex arrangement.

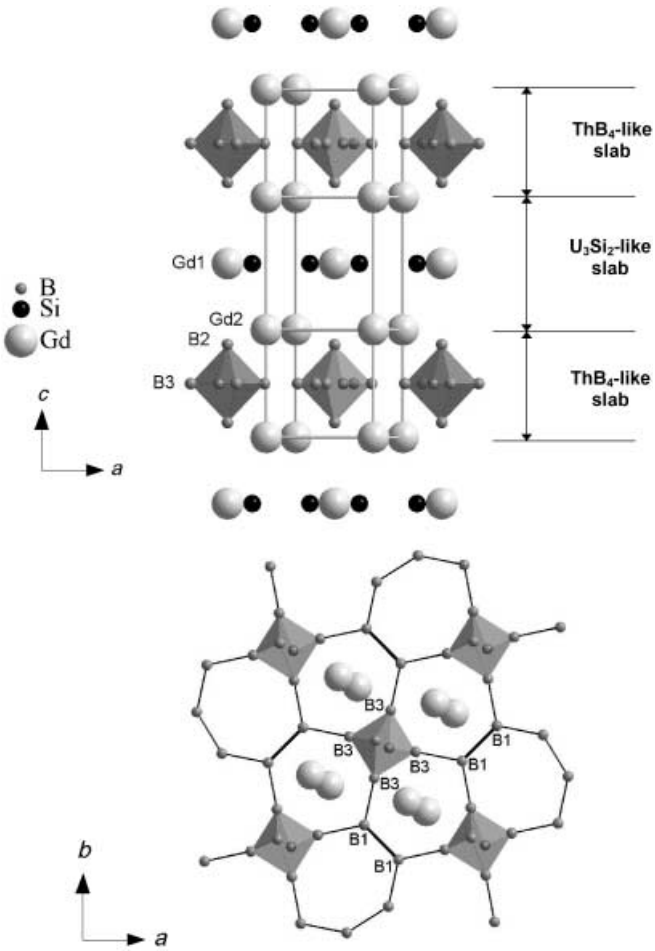

Figure 1. Crystal structure of $Gd_5Si_2B_8$: 3D representation showing the ThB_4-like and U_3Si_2-like slabs, along the [001] direction (top) and a view of the ThB_4-like slab down the *c* axis (bottom).

Magnetic susceptibility and magnetization measurements were performed on the title compound. In the paramagnetic regime, the reciprocal susceptibility data follow a Curie–Weiss law (Figure 2). The derived value of the effective moment leads to $\mu_{eff} = 8.25\,\mu_B$ ($\mu_{eff}^{theor} = 7.94\,\mu_B$) with the paramagnetic Curie temperature $\Theta_p = 50$ K. The absolute values of the real part χ' ($B = 0.001$ T) of the dynamic susceptibility as well as χ_{DC} measured in external fields $B =$ 0.01 T (not shown) and 0.1 T are in good accordance (a weak field dependence is encountered, only). The curves pass pronounced maxima at $T_{N1} = 72$ K and 70 K, respectively, which must be attributed to the onset of antiferromagnetic order of the rare-earth-metal substructure (Figure 2, upper inset). However, the imaginary part χ'' also reveals a rather weak temperature dependency around T_{N1}, which in general is the typical fingerprint of ferro- or ferrimagnetic ordering.

The isothermal magnetization curve versus applied fields at 1.8 K is fully reversible and practically linear up to $B = 2$ T confirming an antiferromagnetic spin alignment at low temperatures and moderate applied magnetic fields (Figure 2, lower inset).

The temperature dependence of the electrical resistivity ρ(T) (Figure 3) which clearly indicates that $Gd_5Si_2B_8$ is

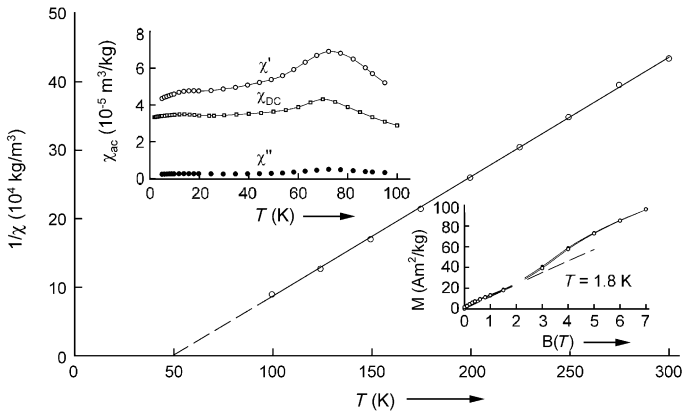

Figure 2. Reciprocal susceptibility versus temperature for $Gd_5Si_2B_8$. Upper inset: temperature dependence of the ac and dc susceptibilities. Lower inset: isothermal magnetization versus applied magnetic field at $T = 1.8$ K (open symbols in increasing fields, filled symbols in decreasing field, dashed line extrapolated linear region).

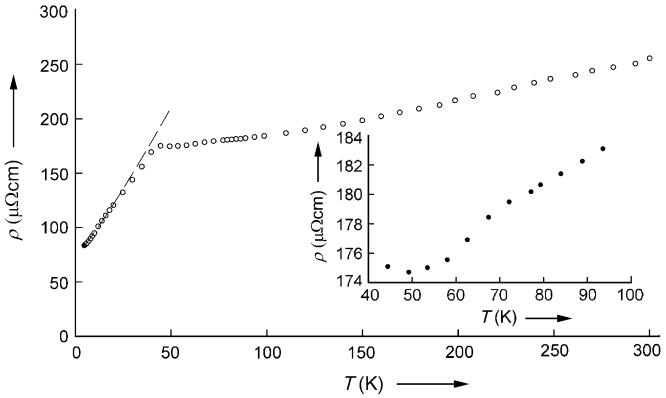

Figure 3. Temperature dependence of the electrical resistivity for $Gd_5Si_2B_8$ (dashed line calculated after $\rho = \rho_o + AT^n$). Inset: reduced scaling.

metallic in character, shows on the other hand a pronounced change of slope at $T_{N2} = 44$ K, which is close to Θ_p. The negative temperature gradient of $\rho(T)$ above the ordering temperature is a clear indication of Brillouin zone (super zone) scattering owing to the onset of antiferromagnetic ordering. Furthermore a less pronounced kink in the $\rho(T)$ plot is observed at $T_{N1} = 72$ K, which corroborates with the magnetic measurements above (Figure 2, upper inset).

The following is concluded: the sample undergoes a weak (canted) ferrimagnetic-like order at T_{N1} followed by a collinear antiferromagnetic spin alignment at T_{N2}. The positive value of Θ_p, however, favoring an overall ferromagnetic coupling of the moments suggests a rather complex spin structure, that is, the two crystallographically different Gd1 and Gd2 atoms eventually form planar ferromagnetic sheets, which are coupled antiparallel inter-plane or, for example, a square-wave modulation of the magnetic moments could be established below $T_{N2} = 44$ K. In the temperature interval $T_{N2} < T < T_{N1}$ a small canting angle of both ferromagnetic substructures might lead to the weak net magnetization, $M = 0.5\ \mu_B$ per formula unit (f.u.), observed at a field of $B = 0.1$ T (ferrimagnetism). The gradual upturn of $M(B)$ in higher fields is reminiscent of a metamagnetic-like transition as shown in the lower inset of Figure 2. The derived value of the ferromagnetic "saturation" moment $\mu_S = 16\ \mu_B$/f.u. at $B = 7$ T is far below the expected value $gJ = 35\ \mu_B$/f.u. in case of collinear ferromagnetic ordering.

In the ordered state, the resistivity follows only a $T^{1.14}$ law (dashed line in Figure 3), which also supports the assumption of a more complex spin structure above when compared with the expected T^{3-4} dependence of isotropic antiferromagnets. Neutron-diffraction experiments have already shown the coexistence of ferromagnetic and antiferromagnetic components in heavy rare-earth silicides[11] and germanides,[12] and recently for Eu_3Si_4.[13]

The assignment of the oxidation states of fragments is a useful starting point to understand the structural arrangement of the non-metal substructure.[5] The isolated Si_2 pairs should satisfy the octet rule, that is, be considered as Si_2^{6-}, with a Si–Si single bond (2.36(2) Å).[14] The favored electron count for the boron octahedra corresponds to B_6^{4-} units.[15] Charge assignment of the B1–B1 units is less straightforward. The B1 atoms are sp^2 hybridized and coplanar. Assuming 2-electron, 2-center bonding (2e–2c), they can either obey the sextet or the octet rule.[15] The sextet rule assumes B1–B1 single bonds and leads to the formal electron partitioning $(Gd^{2+})_5(Si_2^{6-})(B_6^{4-})(B_2)$ which is unlikely for its unrealistic metal oxidation state. The octet rule allows the possibilities for double or single B1–B1 bonds, corresponding to $(Gd^{2.4+})_5(Si_2^{6-})(B_6^{4-})(B_2^{2-})$ and $(Gd^{2.8+})_5(Si_2^{6-})(B_6^{4-})(B_2)^{4-}$, respectively. None of these charge distributions is fully satisfactory, since the first one disagrees somewhat with the rather long B1–B1 separation (1.80(5) Å) whereas in the second one (single bond), a nonplanar, sp^3 hybridization of the $(B1)^{2-}$ atoms is expected.

Nevertheless, in any of the charge partitionings considered above, the metal atoms are not fully oxidized, which suggests metallic behavior as observed experimentally (see Figure 3). This behavior is confirmed by density functional calculations conducted on $Gd_5Si_2B_8$ within the LMTO formalism.[16] The resulting total and projected spin-polarized density of states (DOS) are shown in Figure 4. There is a large participation of the metal 5d orbitals around the Fermi level, but also significant contribution of B and Si orbitals. This situation reflects strong metal–nonmetal covalent interactions. Both spin-up and spin-down 4f states form rather sharp bands separated by approximately 6.5 eV weakly spread out over around 1 eV, which reflect some poor mixing with other Gd orbitals as well as with B and Si orbitals. Except for the 4f states, hardly any polarization of the conduction band is observed.

Crystal orbital Hamiltonian populations (COHP) which indicate energetic contributions of crystal orbitals between orbitals and/or atoms were computed for the different B–B contacts encountered in $Gd_5Si_2B_8$ and compared.[17] It appears that B1–B1 π* antibonding states are occupied as a result of a formal electron transfer from the Si_2 nonbonding electron pairs, which favors the proposed electron distribution $(B_2)^{4-}$. Indeed, rather similar integrated COHP (ICOHP) values of −0.410 and −0.450 Ry/cell are computed for the B1–B1

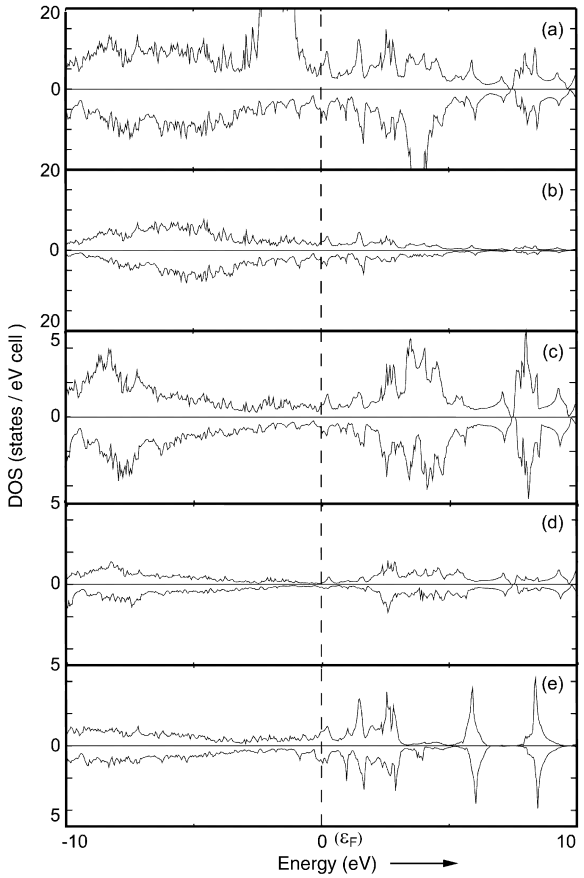

Figure 4. Spin-up and spin-down DOS for $Gd_5Si_2B_8$: a) Total, b) Gd d orbitals, c) B_6 octahedra, d) B_2 units, and e) Si_2 pairs.

(1.80(5) Å) contacts and the B1–B3 (1.78(2) Å) single bonds, respectively. This result is more in favor of a B1–B1 single bond. As expected, the ICOHP values of −0.265 and −0.316 Ry/cell corresponding to the B2–B3 (1.84(3) Å) and B3–B3 (1.81(2) Å) bonds of the octahedra, respectively, imply weaker bonding than in the former B1–B1 and B1–B3 bonds, reflecting their 2e–3c character.

The electron localization function (ELF) which helps to visualize chemists' intuitive ideas of bonding and nonbonding electron pairs in solids and molecules was calculated.[18] The distribution plot of ELF in the (002) plane containing B1 and B3 atoms (Figure 5), shows maxima between B1–B1 (B_2 unit) and also between B1–B3 (B_2 unit–octahedron) and in the center of the $(B3)_4$ square (octahedron). The latter reflects the electron deficiency of the B_6^{4-} octahedra. Integration of the valence electron density gives roughly the same number of electrons for the B1–B1 and B1–B3 bonds, in agreement with the comparable B–B separations experimentally measured and supporting the $(Gd^{2.8+})_5(Si_2^{6-})(B_6^{4-})(B_2)^{4-}$ charge distribution.

In summary, we have realized the synthesis and the characterization of an unprecedented ternary silicide boride which differs strongly from the handful of reported examples.[3,4] Isostructural analogues with Sm, Tb, Dy, and Y[19] have been characterized. There is some uncertainty in the possible electron counts for the boron network, which arises

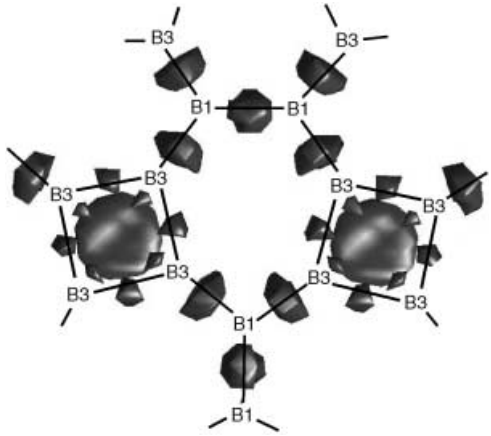

Figure 5. ELF plot in the boron plane for $Gd_5Si_2B_8$ (contour line = 0.73).

from questions of bonding at the B_2 units linking the B_6^{4-} octahedra. Nevertheless, our calculations support a formal electron partitioning B_2^{4-} accounting for the long B1–B1 separations which are experimentally measured. This situation is in contrast to the electron count of B_2^{2-} proposed for the related binary compound GdB_4 in which the corresponding B–B bonds are shorter.[15]

Experimental Section

Suitable amounts of powder and freshly filed chips of the constituents were mixed together and pressed into pellets. The melting of the samples (about 800 mg each) was performed with the help of an arc furnace using a nonconsumable thoriated tungsten electrode under Ti/Zr-gettered argon atmosphere. To ensure homogeneity, the samples were turned over and remelted several times. Finally, to reach thermodynamic equilibrium, the samples were sealed in evacuated silica tubes, heat treated at 1270 K for one month and subsequently quenched in cold water. Single crystals of $Gd_5Si_2B_8$, resulting from a peritectic reaction between GdB_4 and Gd_5Si_3,[7] were obtained by crushing the solidified samples. Energy dispersive spectroscopy (EDS) and wavelength dispersive spectroscopy (WDS) using scanning electron microscopy (Jeol JSM-6400), and electron microprobe analysis (Camebax SX 50) confirmed gadolinium, silicon, and boron as the only components in the samples.[7]

The magnetic properties were studied using a Faraday balance (SUS 10) in the temperature range $80\ K < T < 300\ K$ and in external fields up to 1.3 T and a Lake Shore AC susceptometer (AC 7000, $f =$ 133.3 Hz, $B_{AC} = 1$ mT) for temperatures $4.2\ K \leq T \leq 100\ K$. The dc magnetization was measured in the temperature range 1.8–100 K and in fields up to 7 tesla using a superconducting quantum interference device (SQUID) magnetometer Quantum Design MPMS XL7. Measurements of the electrical resistivity were performed applying a common four-probe Lake Shore ac-resistivity option ($f = 133.3$ Hz, $i = 10$ mA) in the temperature range 4.2–300 K. The alloy buttons were cut into bars of approximately 1 $mm^2 \times 5$ mm using a diamond saw (Bühler Isomet). Electrical contacts were made with commercial silver paint (Degussa, Hanau, Germany) and 25 μm gold wire.

Received: July 24, 2003
Revised: January 14, 2004 [Z52468]

Keywords: boron · density functional theory · gadolinium · magnetic properties · silicon

[1] See, for example: a) Yu. B. Kuz'ma, *Crystallochemistry of borides*, University of L'viv, L'viv, **1983**; b) Yu. B. Kuz'ma, N. F. Chaban, *Binary and Ternary Systems Containing Boron*, Metallurgiya, Moscow, **1990**.

[2] a) F. D. Shepherd, A. C. Yang, *IEDM Tech. Dig.* **1973**, 310; b) L. Pahun, Y. Campidelli, F. Arnaud d'Avitaya, P. A. Badoz, *Appl. Phys. Lett.* **1992**, *60*, 1166; b) Y. Chen, D. A. A. Ohlberg, G. Medeiros-Ribeiro, Y. A. Chang, R. S. Williams, *Appl. Phys. Lett.* **2000**, *76*, 4004; c) J. Y. Duboz, P. A. Badoz, F. Arnaud d'Avitaya, J. A. Chroozek, *Appl. Phys. Lett.* **1989**, *55*, 84.

[3] a) I. Higashi, T. Tanaka, K. Kobayashi, Y. Ishizawa, M. Takami, *J. Solid State Chem.* **1997**, *133*, 11; b) T. Mori, T. Tanaka, *J. Solid State Chem.* **2000**, *154*, 223; c) T. Mori, T. Tanaka, *Mater. Res. Bull.* **2001**, *36*, 2463; d) F. X. Chang, A. Sato, T. Tanaka, *J. Solid State Chem.* **2002**, *164*, 361.

[4] J. R. Salvador, D. Bilc, S. D. Mahanti, M. G. Kanatzidis, *Angew. Chem.* **2002**, *114*, 872; *Angew. Chem. Int. Ed.* **2002**, *41*, 844.

[5] a) P. Rogl, *Phase Diagram of Ternary Metal-Boron-Carbon Systems*, MST International Services, ASM, Stuttgart, **1998**; b) J. Bauer, J.-F. Halet, J.-Y. Saillard, *Coord. Chem. Rev.* **1998**, *178–180*, 723, and references therein; c) J.-F. Halet in *Contemporary Boron Chemistry* (Eds.: M. G. Davidson, A. K. Hugues, T. B. Marder, K. Wade), Royal Society of Chemistry, Cambridge, **2000**, p. 514.

[6] R. Jardin, V. Babizhetskyy, R. Guérin, J. Bauer, *J. Alloys Compd.* **2003**, *353*, 233.

[7] V. Babizhetskyy, J. Roger, S. Députier, R. Jardin, J. Bauer, R. Guérin, *J. Solid State Chem.* **2004**, *117*, 415.

[8] Crystal data for $Gd_5Si_2B_8$: $M_r = 924.42$; tetragonal, space group $P4/mbm$, $a = 7.2665(3)$, $c = 8.2229(7)$ Å, $V = 434.19(4)$ Å^3, $Z = 2$, $\rho_{calcd} = 7.06$, $\mu = 37.82$ mm^{-1}, $R/wR_2 = 4.46/9.74$ % for 259 reflections with $I > 2\sigma(I)$) and 28 parameters, 298 independent reflections ($R_{int} = 4.75$ %), GOF = 1.16. X-ray diffraction data were collected at ambient temperature on a Nonius Kappa CCD X-ray area-detector diffractometer with graphite-monochromatized $Mo_{K\alpha}$ radiation ($\lambda = 0.71073$ Å). The structure was solved by direct methods using the SIR97 program (A. Altomare, M. C. Burla, M. Camalli, B. Carrozzini, G. L. Cascarano, C. Giacovazzo, A. Guagliardi, A. G. G. Moliterni, G. Polidori, R. Rizzi, *Acta Crystallogr. Sect. A* **1999**, *32*, 115 and refined with the SHELXL suite of program (G. M. Sheldrick, SHELXL-97, Programm for the Refinement of Crystal Structures, University of Göttingen, Germany, **1997**). Further details on the crystal structure investigations may be obtained from the Fachinformationszentrum Karlsruhe, 76344 Eggenstein-Leopoldshafen, Germany (fax: (+49) 7247-808-666; e-mail: crysdata@fiz-karlsruhe.de), on quoting the depository number CSD-412944.

[9] A. Zalkin, D. H. Templeton, *Acta Crystallogr.* **1953**, *6*, 269.

[10] a) W. H. Zachariasen, *Acta Crystallogr.* **1949**, *2*, 94; b) K. Remschnig, T. Le Bihan, H. Noël, P. Rogl, *J. Solid State Chem.* **1992**, *97*, 391.

[11] I. P. Semitelou, H. Konguetsof, J. K. Yakinthos, *J. Magn. Magn. Mater.* **1989**, *79*, 131.

[12] P. Schobinger-Papamantellos, *J. Magn. Magn. Mater.* **1982**, *28*, 97.

[13] F. Weitzer, Yu. Prots, W. Schnelle, K. Hiebl, Yu. Grin, *J. Solid State Chem.*, **2004**, accepted.

[14] R. Pöttgen, R.-D. Hoffmann, D. Kussmann, *Z. Anorg. Allg. Chem.* **1998**, *624*, 945.

[15] M. T. Garland, J. P. Wiff, J. Bauer, R. Guérin, J.-Y. Saillard, *Solid State Sci.* **2003**, *5*, 705, and references therein.

[16] Band-structure calculations were performed with the scalar relativistic tight-binding linear muffin–tin orbital method in the atomic spheres approximation (LMTO-ASA) (O. K. Andersen, O. Jepsen, TB-LMTO-ASA47, Stuttgart, Germany, **1996**). Exchange and correlation were treated in the local density approximation using the von Barth–Hedin local exchange correlation potential (U. von Barth, L. Hedin, *J. Phys. C* **1972**, *5*, 1629).

[17] a) R. Dronskowski, P. E. Blöchl, *J. Phys. Chem.* **1993**, *97*, 8617; b) F. Boucher, R. Rousseau, *Inorg. Chem.* **1998**, *37*, 2351.

[18] a) A. D. Becke, N. E. Edgecombe, *J. Chem. Phys.* **1990**, *92*, 5397b) A. Savin, R. Nesper, S. Wengert, T. F. Fässler, *Angew. Chem.* **1997**, *109*, 1892; *Angew. Chem. Int. Ed. Engl.* **1997**, *36*, 1808, and references therein.

[19] Unit cell parameters: $Sm_5Si_2B_8$ ($a = 7.2616(3)$, $c = 8.2260(3)$ Å, $V = 433.76(3)$ Å^3), $Tb_5Si_2B_8$ ($a = 7.2321(2)$, $c = 8.1260(4)$ Å, $V = 425.02(3)$ Å^3), $Dy_5Si_2B_8$ ($a = 7.2205(2)$, $c = 8.0540(3)$ Å, $V = 419.90(2)$ Å^3), and $Y_5Si_2B_8$ ($a = 7.2234(2)$, $c = 8.0961(3)$ Å, $V = 422.40(3)$ Å^3). The crystal structure of $Y_5Si_2B_8$ was recently published: J. Roger, R. Jardin, V. Babizhetskyy, J. Bauer, R. Guérin, *Z. Kristallogr. New Cryst. Struct.* **2003**, *218*, 1.

